INTERNATIONAL JOURNAL OF PRECISION ENGINEERING AND MANUFACTURING Vol. 15, No. 8, pp. 1615-1623 AUGUST 2014 / 1615
DOI: 10.1007/s12541-014-0511-x

Analysis of Dynamic Model of a Top-Loading Laundry Machine with a Hydraulic Balancer

Jung-Soo Cho[1], Hyun-Yong Jeong[1,#], and Kyung-Chul Kong[1]

1 School of Mechanical Engineering, Sogang University, Seoul, South Korea, 121-742
Corresponding Author / E-mail: jeonghy@sogang.ac.kr, TEL: +82-2-705-8640, FAX: +82-2-712-0799

KEYWORDS: Laundry machine, Hydraulic balancer, Newtonian mechanics, Dynamics simulation, Vibration characteristics

This paper analyzes the vibration characteristics of a top-loading-laundry machine with a hydraulic balancer. For numerical simulation of the laundry machine dynamics, its dynamic model is introduced, where ball models are employed to represent the dynamics of a hydraulic balancer. For verification and validation of the established dynamic model, the accelerations of an actual laundry machine are obtained from three-axis accelerometers attached at the upper part and the lower part of a tub respectively. Since the signal-to-noise ratio of the measured acceleration data is small due to the electric noise induced by the driving motor, and a wavelet de-noising method is applied for low-pass filtering without a phase shift. The dynamic model of a top-loading-laundry machine is developed by Newtonian mechanics. From the extensive simulation studies, it turned out that the number of balls, gyration radius of a ball, and damping coefficient between a ball and the basket are the most important three design parameters. The accuracy of the proposed dynamic models is verified based on root-mean-square error and the three design parameters were analyzed. Gyration radius of a ball, which is the most critical parameter, is estimated by the relationship with positions of the unbalanced masses and the dynamic model with the estimated gyration radius of a ball is validated by experiment.

Manuscript received: October 25, 2013 / Revised: March 29, 2014 / Accepted: April 3, 2014

NOMENCLATURE

m = total mass except balls and unbalanced masses
m_u = unbalanced mass
m_h = a ball's mass
a = gyration radius of an unbalanced mass
r = gyration radius of balls
b = height of an unbalanced mass from c.g.
h = height of a ball from c.g.
k = stiffness of suspensions
c = damping coefficient of suspensions
c_h = damping coefficient between balls and the basket

1. Introduction

Laundry machines can be classified into two major groups in terms of the structures and mechanisms; top-loading laundry machines and front-loading laundry machines. Both types have unique advantages and disadvantages in efficiency and/or visual design. In light of vibration transmissibility, i.e., the magnitude of forces transmitted to the ground, which is one of the critical constraints for laundry machines, top-loading laundry machines are more effective than front-loading types because the direction of induced forces is perpendicular to the ground. Due to the precession and whirling of a washing basket as well as an unbalanced mass in the spin drying process, however, the lateral vibration of a top-loading laundry machine is unavoidable. In recent washing machines, therefore, a hydraulic balancer is installed at the rotating basket for suppressing the undesired vibration.[1-3]

A hydraulic balancer at the upper rim of the basket contains salt water. In the spin drying process, as the water of clothes becomes squeezed out, they tend to clump, creating an unbalanced mass in the basket. As the rotating speed of the basket is gradually increased, liquid in the hydraulic balancer deflects automatically to the opposite side of where an unbalanced mass is positioned. With this mechanism, a hydraulic balancer has been considered more effective for vibration suppression of the basket and tub induced by the unbalanced mass than mechanical balancers due to low cost.[4] However, as fluid in the hydraulic

balancer deflects to the same side of the position of an unbalanced mass at the beginning of the spin drying process, the undesired vibration of a top-loading laundry machine induced by the fluid deflection is added to that by an unbalanced mass. For this issue, ideas have been proposed to suppress the initial fluid deflection of a hydraulic balancer. Baffles and plates can be used for the purpose to prevent the initial fluid deflection. Baffles are usually installed inside a hydraulic balancer to block the salt water from passing through but have orifices or openings so that the fluid deflects in a way to reduce the undesirable vibration of the basket at the high rotating speed. It depends on the number and size of baffles that the fluid deflection and the fluid force is in control.[5] The liquid was proven unable to generate a centrifugal force at the low rotating speed of the basket through a baffled CFD hydraulic balancer model, and the size of baffles was optimized by experiments.[6] Besides baffles, installing a middle plate at the outer periphery of a hydraulic balancer can be one of the methods.[7] As baffles have orifices or openings, the middle plate is also a finite length long to the inner side of a hydraulic balancer in order to allow the free motion of liquid at the high rotating speed. However, it is noteworthy that only dynamics of a hydraulic balancer were focused and its boundary conditions were assumed.

Although analyzing a hydraulic balancer itself using the reasonable boundary conditions is meaningful, more importantly, it should be comprehended on how the hydraulic balancer and the mechanical washing system interact to create or reduce the vibration of a top-loading laundry machine. Due to the complexity and inefficiency to realize fluid of a hydraulic balancer in the dynamic simulation, ball balancer models for the hydraulic balancer have been introduced. Studies on ball balancer models have long been conducted for eccentric rotors and optical disk.[8-11] Likewise, ball models were used to describe the effect of an hydraulic balancer, with which the stability analysis and parametric study of a top-loading laundry machine were performed at the steady-state condition.[12-15] In most of the time of the spin drying process, however, a top-loading laundry machine is under transient condition rather than under steady state condition because the rotating speed of the basket varies over time.

The paper proposes dynamic model that conforms to vibration characteristics of a top-loading laundry machine with a hydraulic balancer derived from Newton's law. Parametric study was conducted by tuning the number of balls, gyration radius of balls, and damping coefficient between balls and the basket, where fluid in the hydraulic balancer is described as balls. By rotating speed slope region, the vibration characteristics similarity between the dynamic model and its actual laundry machine was evaluated based on root-mean-square error for six accelerations obtained from the two respective three-axis accelerometers on the upper part and on the lower part of a tub in experiments. Gyration radius of balls was estimated depending on the positions of unbalanced masses combined and the dynamic model with the estimated gyration radius of a ball was validated by experiment.

2. Dynamics of a Top-Loading Laundry Machine

In this section, analysis on the dynamics of a top-loading laundry machine and its equation of motion is introduced.

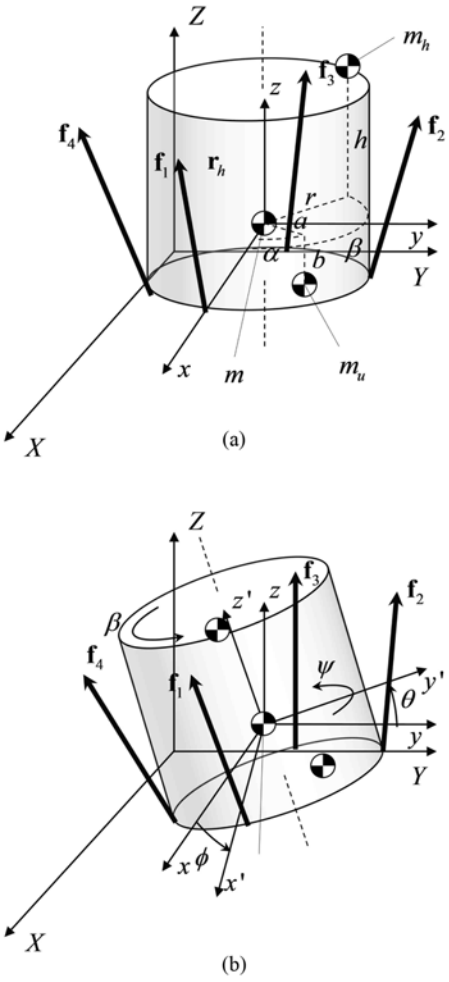

Fig. 1 A tub with a rotating basket; (a) an idle state, (b) a rotated state

Fig. 1 shows the schematic diagram of a tub with a rotating basket. m_u and m_h represent the masses of an unbalanced mass and a hydraulic balancer, respectively. The tub and basket rotate in the three-dimensional space, as shown in Fig. 1(b), where the rotation angles, θ, ϕ, and ψ, represent the rotation about the z-axis of the fixed (inertial) system, the rotation about the x-axis, and the rotation about the z'-axis of the body (rotating) system. The origin for the rotation motion is set to the position of the center of mass of the tub and basket; the position of the center of mass of the tub and basket is denoted by $\mathbf{r}_o$. From the figure that the positions of m_u and m_h are represented as follows.

$$\mathbf{r}_u = \begin{bmatrix} a\cos\alpha \\ a\sin\alpha \\ b \end{bmatrix}, \quad \mathbf{r}_h = \begin{bmatrix} r\cos\beta \\ r\sin\beta \\ h \end{bmatrix} \tag{1}$$

With this setting, the equations of motions of rotation and translation are derived in the following sections.

2.1 Equation of translational motions

The basket and tub are subjected to external forces (e.g., the gravity and spring forces), while hung by four sets of springs and dampers. Notice that the positions of the unbalanced mass and the hydraulic balancer are respectively $\mathbf{r}_o+\mathbf{R}_b^i(\psi, \phi, \theta)\mathbf{r}_u$ and $\mathbf{r}_o+\mathbf{R}_b^i(\psi, \phi, \theta)\mathbf{r}_h$, where $\mathbf{R}_b(\psi, \phi, \theta)$ is the 3×3 rotation matrix corresponding to (ψ, ϕ, θ).

Therefore, the equation of motion of translation[16] is obtained by Newton's second law of motion, i.e.,

$$\begin{aligned}(m+m_u+m_h)\ddot{\mathbf{r}}_o &= \sum_{i=1}^{4}\mathbf{f}_i+(m+m_u+m_h)\mathbf{g}\\ -m_u[(\ddot{\mathbf{r}}_u)_i&+2(\boldsymbol{\omega}_b)_i\times(\dot{\mathbf{r}}_u)_i+(\dot{\boldsymbol{\omega}}_b)_i\times(\mathbf{r}_u)_i+(\boldsymbol{\omega}_b)_i\times(\boldsymbol{\omega}_b)_i\times(\mathbf{r}_u)_i]\\ -m_h[(\ddot{\mathbf{r}}_h)_i&+2(\boldsymbol{\omega}_b)_i\times(\dot{\mathbf{r}}_h)_i+(\dot{\boldsymbol{\omega}}_b)_i\times(\mathbf{r}_h)_i+(\boldsymbol{\omega}_b)_i\times(\boldsymbol{\omega}_b)_i\times(\mathbf{r}_h)_i]\end{aligned} \tag{2}$$

where $\mathbf{g}$ is the gravitational acceleration vector, and $\mathbf{f}_i$'s are the external forces exerted by springs and dampers. Notice that the reaction forces due to the centripetal motion and angular acceleration are involved in the second and third terms of (2).

2.2 Equations of rotational motions

Without the unbalanced mass and the hydraulic balancer, the rotating basket is geometrically symmetric, where the symmetric rotation axis is aligned with z'-axis. Therefore, the moments of inertia of the basket ($\mathbf{I}_{bo}$) is diagonal, i.e.,

$$\mathbf{I}_{bo} = diag(I_{bxx}, I_{byy}, I_{bzz}) \tag{3}$$

where the moment of inertia of the basket includes that of tub, motor, stator, etc. Note that the moment of inertia of the tub about z'-axis is assumed to be zero (i.e., tub is not supposed to rotate about z'-axis). The unbalanced mass and the hydraulic balancer, however, introduce products of inertia, as well as moments of inertia about the principal axes of the basket. Including m_u and m_h, the moment of inertia of the basket is

$$\mathbf{I}_b = \begin{bmatrix} I_{xx} & I_{xy} & I_{xz} \\ I_{xy} & I_{yy} & I_{yz} \\ I_{xz} & I_{xy} & I_{zz} \end{bmatrix} \tag{4}$$

where

$$I_{xx} = I_{bxx}+m_u(a^2\sin^2\alpha+b^2)+m_h(r^2\sin^2\beta+h^2)$$

$$I_{yy} = I_{byy}+m_u(a^2\cos^2\alpha+b^2)+m_h(r^2\cos^2\beta+h^2)$$

$$I_{zz} = I_{bzz}+m_u a^2+m_h r^2$$

$$I_{xy} = -m_u a^2\cos\alpha\sin\alpha-m_h r^2\cos\beta\sin\beta$$

$$I_{yz} = -m_u ab\sin\alpha-m_h rh\sin\beta$$

$$I_{xz} = -m_u ab\cos\alpha-m_h rh\cos\beta$$

For the definition of angular momentum of the basket, the angular velocity is necessary. The basket is rotated by ψ about the z'-axis in the rotating coordinate system, and thus the components of angular velocity of the basket, $\boldsymbol{\omega}_b$, is

$$\boldsymbol{\omega}_b = \begin{bmatrix} \cos\psi\cos\phi & \sin\psi & 0 \\ -\sin\psi\cos\phi & \cos\psi & 0 \\ \sin\phi & 0 & 1 \end{bmatrix} \begin{bmatrix} \dot{\theta} \\ \dot{\phi} \\ \dot{\psi} \end{bmatrix} \tag{5}$$

The rotation about the symmetric axis is often called a *spin*; the spin of the basket is defined as $S := \omega_{bz'} = \dot{\theta}\sin\phi + \dot{\psi}$.

From (4) and (5), angular momentum of the basket is defined as

$$\mathbf{L}_b = \mathbf{I}_b\boldsymbol{\omega}_b \tag{6}$$

In the rotating coordinate system, the equation of motion for rotation[16] is

$$\mathbf{T} = \frac{d\mathbf{L}_b}{dt}+\boldsymbol{\omega}_b\times\mathbf{L}_b \tag{7}$$

where $\mathbf{T}$ is the moments due to external forces and the gravity, i.e., where $\mathbf{R}_b^i(\psi, \phi, \theta)$ is the rotation matrix that converts the reference (fixed) coordinate system into the rotating coordinate system. $\mathbf{r}_{fi}$'s are the vectors that indicate the position of springs and dampers in the reference coordinate system (see Fig. 1(b)), and $\mathbf{f}_i$'s are the forces due to the springs and dampers. $\mathbf{T}_a := [0\ \ 0\ \ \tau]^T$ is an actuation torque that an electric motor generates to rotate the basket. The second term in (8) represents the spring and damping forces, the third term means a moment due to the gravity, and the fourth and fifth terms indicate the centripetal forces induced by the unbalanced mass and hydraulic balancer.

$$\begin{aligned}\mathbf{T} = \mathbf{T}_a&+\mathbf{R}_i^b(\psi,\phi,\theta)\sum_{i=1}^{4}\mathbf{r}_{fi}\times\mathbf{f}_i+m_u\mathbf{r}_u\times\mathbf{R}_i^b(\psi,\phi,\theta)\\ &[\mathbf{g}-\ddot{\mathbf{r}}_o-(\ddot{\mathbf{r}}_u)_i-2(\boldsymbol{\omega}_b)_i\times(\dot{\mathbf{r}}_u)_i-(\boldsymbol{\omega}_b)_i\times(\boldsymbol{\omega}_b)_i\times(\mathbf{r}_u)_i]+m_h\mathbf{r}_h\\ &\times\mathbf{R}_i^b(\psi,\phi,\theta)[\mathbf{g}-\ddot{\mathbf{r}}_o-(\ddot{\mathbf{r}}_h)_i-2(\boldsymbol{\omega}_b)_i\times(\dot{\mathbf{r}}_h)_i-(\boldsymbol{\omega}_b)_i\times(\boldsymbol{\omega}_b)_i\times(\mathbf{r}_u)_i]\\ &+c_h\dot{\beta}\mathbf{e}_z\end{aligned} \tag{8}$$

The hydraulic balancer rotates on the rotating basket, which indicates the hydraulic balancer rotates in one-dimensional space, where the rotation angle β represents the rotation about z'-axis. The angular momentum of the hydraulic balancer is defined as

$$L_h = I_h\dot{\beta} \tag{9}$$

where $I_h = m_h r^2$ is the moment of inertia of the hydraulic balancer about z'-axis.

In the rotating coordinate system, the equation of rotational motion[16] for the hydraulic balancer is

$$\begin{aligned}\frac{dL_h}{dt}+\dot{\beta}\times L_h &= \mathbf{e}_z\cdot(m_h\mathbf{r}_h\times\mathbf{R}_i^b(\psi,\phi,\theta)\\ &[\mathbf{g}-\ddot{\mathbf{r}}_o-(\dot{\boldsymbol{\omega}}_b)_i\times(\mathbf{r}_h)_i-(\boldsymbol{\omega}_b)_i\times(\boldsymbol{\omega}_b)_i\times(\mathbf{r}_h)_i])-c_h\dot{\beta}\end{aligned} \tag{10}$$

where the right terms in (10) are the moments due to external forces and the gravity. Note that $\mathbf{e}_z$ is a unit vector for the rotating axis of the hydraulic balancer and c_h is the damping coefficient between the hydraulic balancer and the basket.

2.2.1 Rotation matrix

In this section, the rotation matrix and the coordinate translations are covered. Consider the four coordinate systems. The coordinate system denoted as i represents the inertial frame, 1 represents the system rotated about x-axis of inertial frame, the system 2 is rotated about y'-axis of the system 1, and the system b is rotated about 3-axis of the system 2. The order of the coordinate rotation is important, and with the above rotation sequence the rotation matrices are as below.

$$\begin{bmatrix} x \\ y' \\ z' \end{bmatrix}_1 = \begin{bmatrix} 1 & 0 & 0 \\ 0 & \cos\theta & \sin\theta \\ 0 & -\sin\theta & \cos\theta \end{bmatrix} \begin{bmatrix} x \\ y \\ z \end{bmatrix} \tag{11}$$

$$\begin{bmatrix} x' \\ y' \\ 3 \end{bmatrix}_2 = \begin{bmatrix} \cos\phi & 0 & -\sin\phi \\ 0 & 1 & 0 \\ \sin\phi & 0 & \cos\phi \end{bmatrix} \begin{bmatrix} x \\ y' \\ z' \end{bmatrix} \tag{12}$$

$$\begin{bmatrix} 1 \\ 2 \\ 3 \end{bmatrix}_b = \begin{bmatrix} \cos\psi & \sin\psi & 0 \\ -\sin\psi & \cos\psi & 0 \\ 0 & 0 & 1 \end{bmatrix} \begin{bmatrix} x' \\ y' \\ 3 \end{bmatrix} \tag{13}$$

2.2.2 Coordinate translation

In (11), $\mathbf{R}_i^1$ translates the *xyz*-axis coordinate to *xy′z′*-axis rotated about θ.

$$1 \underset{\mathbf{R}_i^1}{\overset{\mathbf{R}_1^i}{\rightleftharpoons}} i$$

where

$$\mathbf{R}_i^1 = (\mathbf{R}_1^i)^{-1}$$

Multiple translations are simply multiplying rotation matrices in front of the object coordinate, and the sequence of matrix multiplication is important.

$$b \underset{\mathbf{R}_2^b}{\overset{\mathbf{R}_b^2}{\rightleftharpoons}} 2 \underset{\mathbf{R}_1^2}{\overset{\mathbf{R}_2^1}{\rightleftharpoons}} 1 \underset{\mathbf{R}_i^1}{\overset{\mathbf{R}_1^i}{\rightleftharpoons}} i$$

then

$$b \underset{\mathbf{R}_2^b\mathbf{R}_1^2\mathbf{R}_i^1}{\overset{\mathbf{R}_1^i\mathbf{R}_2^1\mathbf{R}_b^2}{\rightleftharpoons}} i$$

Therefore the rotation matrix which translate *i*-frame to *b*-frame can be represented as a combined matrix.

$$\mathbf{R}_i^b = \begin{bmatrix} c\psi c\phi & s\psi c\theta - c\psi s\phi s\theta & s\psi s\theta + c\psi s\phi c\theta \\ -s\psi c\phi & c\psi c\theta + s\psi s\phi s\theta & c\psi s\theta - s\psi s\phi c\theta \\ s\phi & -c\phi s\theta & c\phi s\theta \end{bmatrix} \tag{14}$$

2.2.3 Angular velocity

The angular velocity of basket is represented in body frame,

$$\begin{aligned} \boldsymbol{\omega}_b &= \begin{bmatrix} \omega_x \\ \omega_y \\ \omega_z \end{bmatrix}_b = \mathbf{R}_2^b\mathbf{R}_1^2 \begin{bmatrix} \dot{\theta} \\ 0 \\ 0 \end{bmatrix} + \mathbf{R}_2^b \begin{bmatrix} 0 \\ \dot{\phi} \\ 0 \end{bmatrix} + \begin{bmatrix} 0 \\ 0 \\ \dot{\psi} \end{bmatrix} \\ &= \begin{bmatrix} \cos\psi\cos\phi & \sin\psi & 0 \\ -\sin\psi\cos\phi & \cos\psi & 0 \\ \sin\phi & 0 & 1 \end{bmatrix} \begin{bmatrix} \dot{\theta} \\ \dot{\phi} \\ \dot{\psi} \end{bmatrix} \end{aligned} \tag{15}$$

2.2.4 Angular momentum

In the previous section, the relationship of rotation matrix and coordinate systems was introduced, and with those information angular momentums in body frame and inertial frame can be defined as below.

$$\mathbf{L}_b = \mathbf{R}_i^b\mathbf{L}_i \qquad \mathbf{L}_i = \mathbf{R}_b^i\mathbf{L}_b \tag{16}$$

$$\boldsymbol{\omega}_b = \mathbf{R}_i^b\boldsymbol{\omega}_i \qquad \boldsymbol{\omega}_i = \mathbf{R}_b^i\boldsymbol{\omega}_b \tag{17}$$

To get the derivative of angular momentum, we take the chain rule on (16),

$$\dot{\mathbf{L}}_i = \mathbf{R}_b^i\dot{\mathbf{L}}_b + \dot{\mathbf{R}}_b^i\mathbf{L}_b \tag{18}$$

and from (6),

$$\dot{\mathbf{L}}_i = \mathbf{R}_b^i\dot{\mathbf{L}}_b + \boldsymbol{\omega}_i \times \mathbf{L}_i = \mathbf{R}_b^i\dot{\mathbf{L}}_b + \tilde{\boldsymbol{\omega}}_i\mathbf{L}_i \tag{19}$$

where

$$\tilde{\boldsymbol{\omega}}_i = \begin{bmatrix} 0 & -\omega_{iz} & \omega_{iy} \\ \omega_{iz} & 0 & -\omega_{ix} \\ -\omega_{iy} & \omega_{ix} & 0 \end{bmatrix} \tag{20}$$

The same process can be applied to $\mathbf{L}_b$,

$$\begin{aligned} \dot{\mathbf{L}}_b &= \mathbf{R}_i^b\dot{\mathbf{L}}_i + \dot{\mathbf{R}}_i^b\mathbf{L}_i = \mathbf{R}_i^b\dot{\mathbf{L}}_i - \boldsymbol{\omega}_b \times \mathbf{L}_b = \mathbf{R}_i^b\dot{\mathbf{L}}_i - \tilde{\boldsymbol{\omega}}_b\mathbf{L}_b \\ &= \mathbf{R}_i^b\dot{\mathbf{L}}_i - \tilde{\boldsymbol{\omega}}_b\mathbf{I}_b\boldsymbol{\omega}_b = \mathbf{M}_b - \tilde{\boldsymbol{\omega}}_b\mathbf{I}_b\boldsymbol{\omega}_b \end{aligned} \tag{21}$$

where $\mathbf{M}_i$ is the rotational net torque in inertial frame, and $\mathbf{M}_b = \mathbf{R}_i^b\mathbf{M}_i$ is in the body frame.

2.2.5 Angular acceleration

For constant body-axis inertia matrix, the derivative of angular momentum is $\dot{\mathbf{L}}_b = \mathbf{I}_b\dot{\boldsymbol{\omega}}_b$,

$$\dot{\mathbf{L}}_b = \mathbf{I}_b\dot{\boldsymbol{\omega}}_b = \mathbf{M}_b - \tilde{\boldsymbol{\omega}}_b\mathbf{I}_b\boldsymbol{\omega}_b \tag{22}$$

then

$$\dot{\boldsymbol{\omega}}_b = \mathbf{I}_b^{-1}(\mathbf{M}_b - \tilde{\boldsymbol{\omega}}_b\mathbf{I}_b\boldsymbol{\omega}_b) \tag{23}$$

3. Simulations

A dynamic model of a top-loading-laundry machine with a hydraulic balancer was built in the previous section. Since in the dynamic model the hydraulic balancer was replaced by the ball balancer, which is a mechanical system much simpler to be modeled than a liquid-filled system, there are three design parameters to be tuned; The number of balls, the gyration radius of balls, and the damping coefficient between balls and the basket. Each parameter was divided into three levels, and the model properties were measured directly or estimated from its CAD model. Table 1 shows design parameters of the dynamic model, respectively. Simulations were carried out and evaluated by a methodology based on root-mean-square error that will be introduced in the latter section.

Table 1 Design parameters of dynamic model of a top-loading laundry machine with a hydraulic balancer

Parameters			
Number of balls	2	3	4
Gyration radius of a ball (mm)	13.2	26.4	2.8
Damping coefficient between a ball and the basket ($Nmsrad^{-1}$)	0.1	0.25	2.0

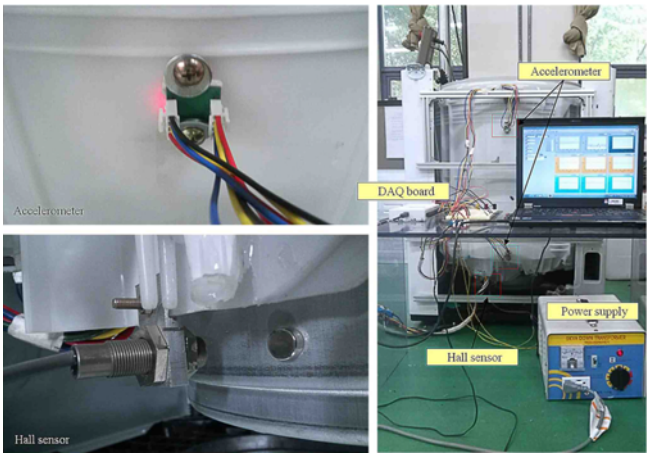

Fig. 2 Experimental set-up; an accelerometer (left-top), a hall sensor (left-bottom)

4. Experiments

The experiment should be carried out in order to be used reference for simulation. In the experiment, accelerations on the upper part and the lower part of a tub were measured during the entire spinning cycle. The accumulated data were effectively noise-reduced by the wavelet transform.

4.1 Experimental set-up

Two accelerometers were used to measure the vibration characteristics of a top-loading-laundry machine. One was installed on the upper part of a tub and the other on the lower part. The hall sensor was installed on the motor that rotates during the spinning cycle in order to measure revolutions of a basket per a sampling time. Data obtained from the hall sensor were applied in the simulation. Accelerometers and a hall sensor were connected to data acquisition (DAQ) board from National Instrument. The sampling time was set to 1ms. The detailed experimental settings are displayed in Fig. 2. The experiments were divided into four cases. The first case was a 1.2 kg unbalanced mass fixed on the lower part of a basket, the second case a 1.0 kg on the lower part and 0.2 kg unbalanced mass the same side on the upper part, the third case a 1.0 kg on the lower part and 0.2 kg unbalanced mass the opposite side on the upper part, and the fourth case both a 1.0 kg and 0.2 kg unbalanced mass arranged on the lower part and on the upper part of a basket respectively at a right angle viewed down from the top, as shown in Fig. 3. The first three cases (see Figs. 3(a), 3(b), 3(c)) were used to propose a dynamic model of a top-loading-laundry machine and the last (see Fig. 3(d)) to validate the dynamic model proposed by the first three experiments.

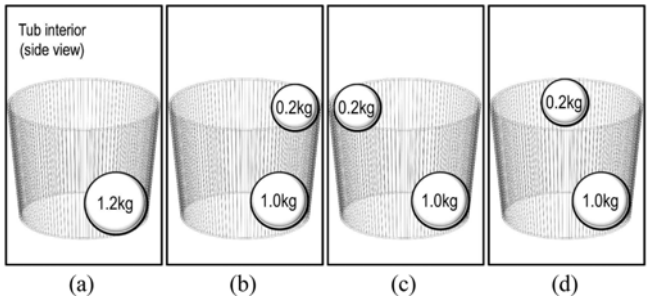

Fig. 3 Positions of unbalanced mass; (a) 1.2 kg mass at the lower part, (b) 0.2 kg mass at the upper part above 1.0 kg mass at the lower part, (c) 0.2 kg mass at the upper part above across 1.0 kg mass at the lower part, (d) 0.2 kg mass at the upper part above 1.0 kg mass at the lower part at a right angle

4.2 Noise Reduction

The raw data obtained directly from accelerometers were so noisy. The noise should be reduced properly to have reliable results from the experiment. There are many methods for noise reduction. For many signals, the low-frequency component is the most important part. Since it gives the signal its identity and most noises include high frequency component, low-pass filters have been frequently used. Especially in case of filtering accumulated data, zero-phase low-pass filters can be preferably applied.

To design a low-pass filter its cut-off frequency should be determined by the engineer. Fourier transform is extremely useful to discover the frequency component of the signal and helps the engineer determine a proper cut-off frequency. However, Fourier transform has a serious drawback. In transforming the entire signal to the frequency domain, time information is lost. If a signal does not change much over time - that is, if it is what is called a stationary signal - this drawback is not very important. However, most interesting signals contain numerous non-stationary or transitory characteristics; drift, trends, abrupt changes, and beginnings and ends of events. These characteristics are often the most important part of the signal. Fourier transform is not suited to detecting them. On the other hand, wavelet transform allows the use of long time intervals where more precise low frequency information is required, and shorter regions where high frequency information is required. Wavelet transform decomposes an interesting signal through low-pass filters and high-pass filters. These decomposed signals are decomposed repeatedly until it reaches the set level.[18] The desired de-noised signal is reconstructed, discarding portion of the decomposed signals through threshold.

Discrete wavelet that Meyer had created was adopted and decomposition level was 5. SURE criterion was used for the suitable number of levels to reconstruct signals and threshold value was properly hand-tuned monitoring the de-noised signals.

5. Analysis

A dynamic model of a top-loading-laundry machine with a hydraulic balancer was built and simulated by tuning three design parameters and experimental data were obtained in the previous section. In this section,

an evaluation methodology to show how similar in vibration characteristics the actual laundry machine and its dynamic model are is introduced and the effects of the three design parameters are discussed with results.

5.1 Evaluation methodology

The adequacy of the dynamic model is to be evaluated when parameters tuned in the dynamic model. Accelerations can be useful for representing vibrations.[17] Since the root-mean-square error is a frequently used measure of the difference between accelerations predicted by a dynamic model and those actually observed in the experiment, it will be a good choice for evaluation.

In the experiment, two three-axis acceleration data and rotating speed data were obtained from two accelerometers and a hall sensor. Although acceleration data were properly de-noised by the wavelet transform, the direct root-mean-square error calculation between experimental accelerations and simulated accelerations may not be appropriate because the root-mean-square error is very sensitive to phase shift between data. Windowing and averaging of a given interval of data will be helpful to calculate the root-mean-square error. Uniform windows were distributed every given time interval of data for both experiments and simulations. The average amplitude was calculated window by window, which represents a single data point for a group of the sampling data included over a window. Thus, the root-mean-square error of experimental and simulated average amplitudes becomes much less sensitive to phase shift. The sensitivity depends on how large the size of a window is. If the size of a window is large, root-mean-square error is less sensitive to phase shift of data than that from when the size of a window is small, but reliability of evaluation methodology may be degraded. Therefore, a window used in this paper is 1000 samplings, i.e., 1 second wide enough to cover the low frequency range. Acceleration data about *xyz*-axis are different such that each should be normalized with its corresponding one in the experiment. Normalized root-mean-square error of window average amplitudes is

$$e_{norm} = \frac{\sqrt{E[(w_{exp} - w_{sim})^2]}}{E[(w_{exp})^2]} \tag{24}$$

Since the total six root-mean-square errors in (24) are hard to analyze and compare similarity of vibration characteristics, a unitary evaluation criterion should be defined as

$$e_{total} = \sqrt{E[(e_{norm})^2]} \tag{25}$$

In order to analyze similarity of vibration characteristics between the actual laundry machine and its dynamic model more effectively, regions are divided into three regions in terms of a rotating speed slope; initial preparatory region, gradual-surging rotating speed region, which is called *Region I* that represents a transient region and constant high rotating speed region, which is called *Region II* that represents a steady-state region as shown in Fig. 4. The initial preparatory region is not considered in this paper. Figs. 5 and 6 show performance map expressed by evaluation criterion e_{total} in order to analyze the effect of the three design parameters; number of balls, gyration radius of a ball, and damping coefficient between a ball and the basket.

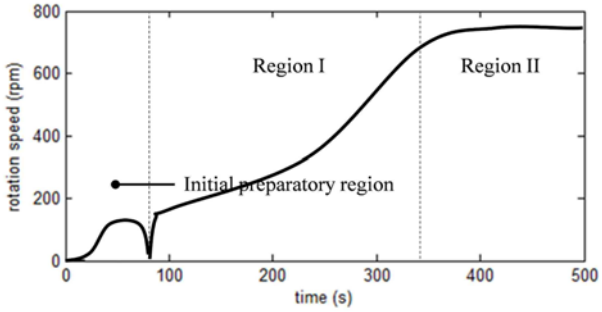

Fig. 4 Rotating speed profile of a top-loading laundry machine: (from left) initial preparatory region, gradual-surging rotating speed region (transient state), and constant high rotating speed region(steady state)

5.2 Effect of design parameters

5.2.1 Number of balls

The number of balls has been considered closely related to the degrees of freedom of fluid in the hydraulic balancer, which means the more balls the closer the characteristics of a ball balancer to those of a hydraulic balancer. If the number of balls is more than two, however, it affects little in vibration characteristics of the dynamic model as displayed in Figs. 5 and 6.

5.2.2 Gyration radius of balls

Gyration radius of balls can be regarded as the extent of liquid deflection in the hydraulic balancer. The larger gyration radius of balls is, the more liquid deflection is assumed to occur in the hydraulic balancer. In the first and second cases, e_{total} is the smallest when gyration radius of balls is 26.4 mm, while when gyration radius of balls is 13.2 mm in the third case. These phenomena can be interpreted as relatively larger liquid deflection in the hydraulic balancer required in the first and second cases compared to in the third case since unbalanced masses are biased. Gyration radius of balls is related with not just the center of mass but the mass moment of inertia of the balancer. For a given gyration radius of balls, the mass moment of inertia remains constant while the center of mass varies, i.e., the two different gyration radii of balls can create the same center of mass, but cannot create the same mass moment of inertia. The smaller gyration radius of balls is, the smaller mass moment of inertia is. To illustrate, e_{total} of the dynamic model with a smaller gyration radius of balls is least in the third case in contrast with in the first and second cases in Figs. 5 and 6. Since liquid in the hydraulic balancer is shapeless, it can have various mass moments of inertia, depending on the vibration amplitudes of the laundry machine. In case of the unbalanced masses distributed, liquid in the hydraulic balancer tends to have less mass moment of inertia than in case of the unbalanced masses biased.

5.2.3 Damping coefficient between balls and the basket

Salt water is generally used as liquid in hydraulic balancers. Though salt water is well-known as extremely low viscous, baffles and orifices in the hydraulic balancer are able to produce viscous damping force by preventing or detouring water from moving freely. In this regard, damping coefficient between balls and the basket was introduced to substitute the effect of baffles and orifices in the hydraulic balancer.

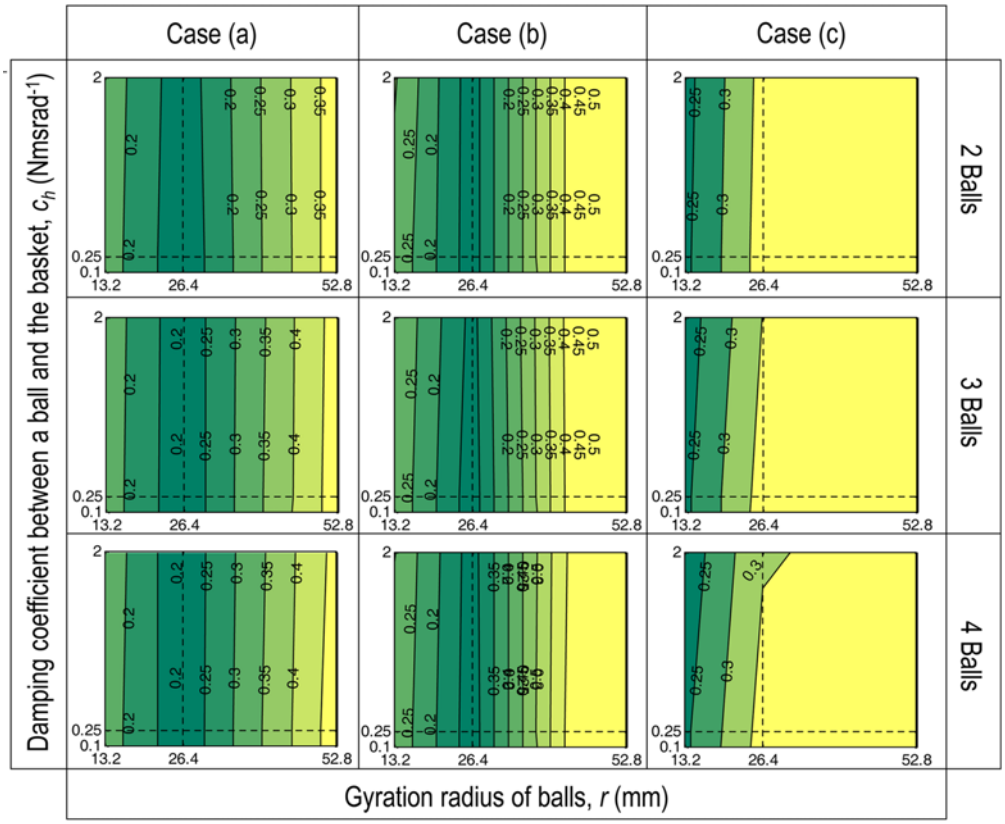

Fig. 5 Performance map in *Region I*; the effect of the three design parameters - number of balls, gyration radius of a ball, and damping coefficient between a ball and the basket)

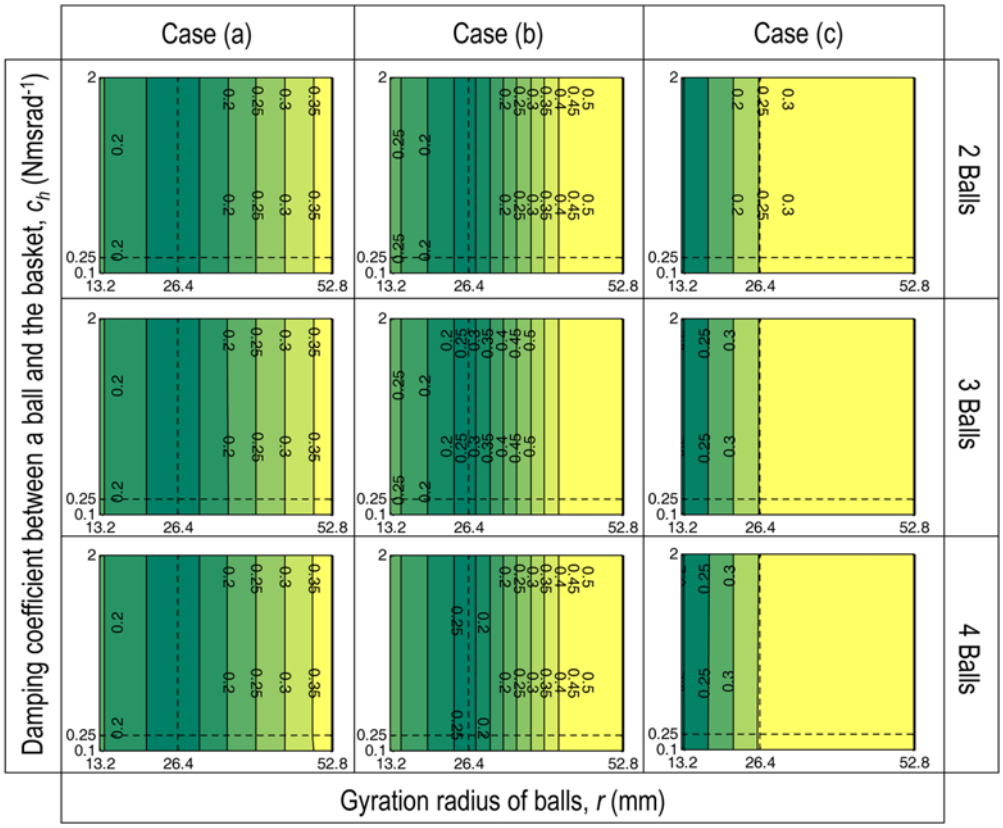

Fig. 6 Performance map in *Region II*; the effect of the three design parameters - number of balls, gyration radius of a ball, and damping coefficient between a ball and the basket)

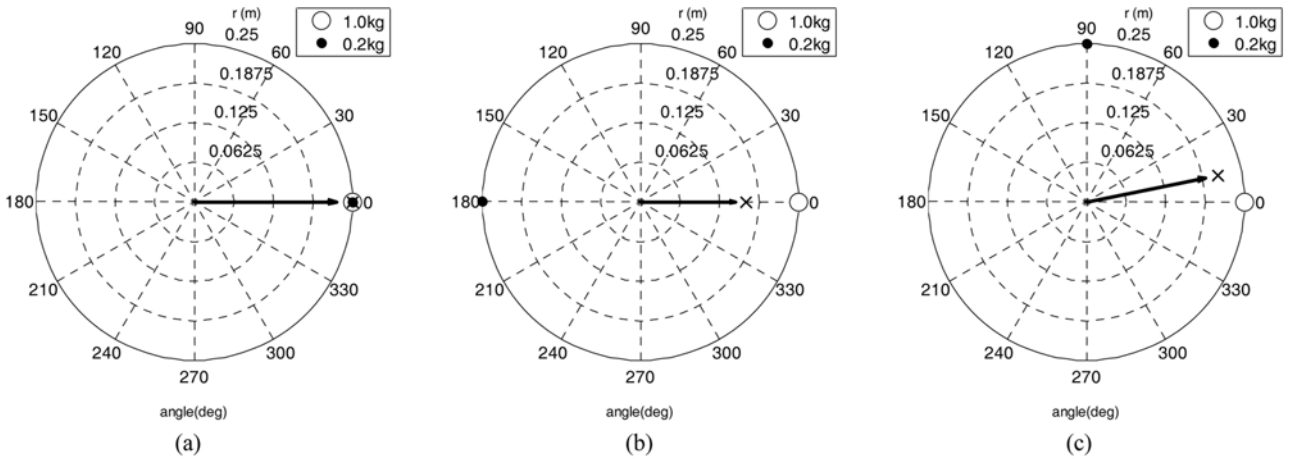

Fig. 7 Center of the unbalanced masses depending on their positions; (a) 0° angle between two different unbalanced masses, (b) 180° angle between two different unbalanced masses, (c) 90° angle between two different unbalanced masses

However, the damping coefficient has almost little influence on vibration characteristics as the number of balls does.

6. Validation

By case, the properly-tuned dynamic models are sorted out, where one is a dynamic model with gyration radius of balls 26.4 mm for the first and second cases where unbalanced mass are biased, and the other a dynamic model with gyration radius of balls 13.2 mm for the third case where unbalanced mass are distributed. Therefore, it should be expected that positions of unbalanced masses are closely related to gyration radius of balls.

As positions of unbalanced masses can be represented by their center of mass, Fig. 7 illustrates center of the unbalanced masses varies depending on their positions, in which each deployment represents a certain case of experiments. For example, Fig. 7(a) represents the first and second cases where unbalanced masses are biased to one side (see Figs. 3(a), 3(b)), Fig. 7(b) represents the third case where unbalanced masses are on the complete opposite of each other (see Fig. 3(c)), and Fig. 7(c) represents the fourth case where unbalanced masses are away at a right angle (see Fig. 3(d)). Note that the vertical distribution of the unbalanced masses affects little in deciding center of the unbalanced masses even though center of the unbalanced masses is not only depending on the horizontal distribution but also vertical distribution because the same gyration radii of balls gave good performance in both the first and second case where masses are all on the lower part or distributed vertically as shown in Figs. 5 and 6.

The dynamic model with the gyration radius of balls of 26.4 mm agrees well with its physical model when the distance from the origin to the center of the unbalanced masses is 250 mm while the dynamic model with the gyration radius of balls of 13.2 mm agrees well with its physical model when the distance from the origin to the center of the unbalanced masses is 167 mm, i.e., the longer the distance from the origin to the center of the unbalanced masses is, the larger gyration radius of balls is needed. Furthermore, they can be assumed linear-proportional through the origin since gyration radius of balls goes to zero due to no unbalanced mass biased if the center of the unbalanced masses is assigned at the origin.

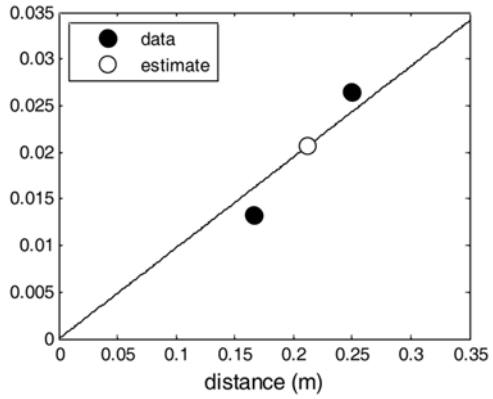

Fig. 8 Estimation of gyration radius of a ball for the fourth case

Table 2 Similarity percentage (%S) = $(1 - e_{total}) \times 100\%$

Case	Region I	Region II
a	83.7%S	83.8%S
b	82.8%S	82.9%S
c	81.0%S	85.4%S
d	87.6%S	89.0%S

Fig. 8 shows linear-proportional relationship between distance from the origin to the center of the unbalanced masses and gyration radius of balls through least-squares method, with which the gyration radius of balls with regard to the center of the unbalanced masses was estimated, simulated, and validated by the fourth experiment (see Fig. 3(d)). Data represent the results from the previous experiments and those from first two experiments are overlaid by calculating center of the unbalanced masses. Thus, similarity percentage of the dynamic model with the estimated gyration radius of balls of 21.0 mm is analogous to the rest of the previous dynamic models, as shown in Table 2. Note that the number of balls and the damping coefficient between balls and the basket used in the simulation were set to 3 and 0.25 $Nmsrad^{-1}$, respectively.

7. Conclusions

Dynamic model of a top-loading laundry machine with a hydraulic balancer was built by Newton's law and tuned by three design parameters such as number of balls, gyration radius of balls, and damping coefficient between a ball and the basket. As dynamic models were evaluated by a newly-developed criterion based on the root-mean-square error, the gyration radius of balls turned out to be the most influential factor in vibration characteristics of the dynamic model, while the number of balls and the damping coefficient between a ball and the basket had little effect. Although vibration characteristics of a dynamic model agree with those of its physical model in both region I and region II for a given case, different dynamic models should be used to describe vibration characteristics of the physical model by case. Finally, the dynamic model of which the gyration radius of balls was estimated depending on the positions of unbalanced masses was validated by an experiment. It is certain that this approach will provide engineers with a guide to design a proper dynamic model corresponding to its physical model.

ACKNOWLEDGEMENT

The financial and technical supports provided by LG Electronics are appreciated. Technical support in setting up experiments provided by Inyong Kwak, a graduate student of Sogang University, is also appreciated.

REFERENCES

1. Kim, D. W., "Clothes Washing Machine with Balancing Device," US Patent, No. 5782110A, 1998.
2. Southworth D. W., Farrington, E. K., and Garstecki, G. M., "Dynamic Balancer for an Automatic Washer," US Patent, No. 6550292B1, 2003.
3. Kim, D. W. and Shin, S. J., "Washing Machine with Ball Balancer," US Patent, No. 58063496A, 1998.
4. Conrad, D. C., "The Fundamentals of Automatic Washing Machine Design based upon Dynamic Constraints," Ph.D. Thesis, School of Mechanical Engineering, Purdue University, 1994.
5. Jung, C. H., Kim, J. T., and Choi, Y. H., "A Computational Study on the Flow Characteristics of a Self-Compensating Liquid Balancer," Journal of Mechanical Science and Technology, Vol. 25, No. 6, pp. 1465-1474, 2011.
6. Son, S. H., Lee, S. B., and Choi, D. H., "Experiment-based Design Optimization of a Washing Machine Liquid Balancer for Vibration Reduction," Int. J. Precis. Eng. Manuf., Vol. 13, No. 8, pp. 1433-1438, 2012.
7. Jung, C. H., Kim, C. S., and Choi, Y. H., "A Dynamic Model and Numerical Study on the Liquid Balancer used in an Automatic Washing Machine," Journal of Mechanical Science and Technology, Vol. 22, No. 9, pp. 1843-1852, 2008.
8. Kim, W., Lee, D. J., and Chung, J., "Three-Dimensional Modelling and Dynamic Analysis of an Automatic Ball Balancer in an Optical Disk Drive," Journal of Sound and Vibration, Vol. 285, No. 3, pp. 547-569, 2005.
9. Green, K., Champneys, A., and Friswell, M., "Analysis of the Transient Response of an Automatic Dynamic Balancer for Eccentric Rotors," International Journal of Mechanical Sciences, Vol. 48, No. 3, pp. 274-293, 2006.
10. Green, K., Champneys, A., Friswell, M., and Muñoz, A., "Investigation of a Multi-Ball, Automatic Dynamic Balancing Mechanism for Eccentric Rotors," Philosophical Transactions of the Royal Society A: Mathematical, Physical and Engineering Sciences, Vol. 366, No. 1866, pp. 705-728, 2008.
11. Lu, C. J., Wang, M. C., and Huang, S. H., "Analytical Study of the Stability of a Two-Ball Automatic Balancer," Mechanical Systems and Signal Processing, Vol. 23, No. 3, pp. 884-896, 2009.
12. Bae, S., Lee, J. M., Kang, Y. J., Kang, J. S., and Yun, J. R., "Dynamic Analysis of an Automatic Washing Machine with a Hydraulic Balancer," Journal of Sound and Vibration, Vol. 257, No. 1, pp. 3-18, 2002.
13. Chen, H. W., Zhang, Q. J., and Fan, S. Y., "Study on Steady-State Response of a Vertical Axis Automatic Washing Machine with a Hydraulic Balancer using a New Approach and a Method for Getting a Smaller Deflection Angle," Journal of Sound and Vibration, Vol. 330, No. 9, pp. 2017-2030, 2011.
14. Chen, H. W. and Zhang, Q. J., "Stability analyses of a Vertical Axis Automatic Washing Machine with a Hydraulic Balancer," Mechanism and Machine Theory, Vol. 46, No. 7, pp. 910-926, 2011.
15. Chen, H. W., Ji, W. X., Zhang, Q. J., Cao, Y., and Fan, S. Y., "A Method for Vibration Isolation of a Vertical Axis Automatic Washing Machine with a Hydraulic Balancer," Journal of Mechanical Science and Technology, Vol. 26, No. 2, pp. 335-343, 2012.
16. Hibbeler, R. C., "Engineering Mechanics: Dynamic SI Package," Pearson Prentice Hall, 11th Ed., pp. 366-374, 2007.
17. Spelta, C., Previdi, F., Savaresi, S. M., Fraternale, F., and Gaudiano, N., "Control of Magnetorheological Dampers for Vibration Reduction in a Washing Machine," Mechatronics, Vol. 19, No. 3, pp. 410-421, 2009.
18. Misiti, M., Misiti, Y., Goerges, O., and Jean-Michel, P., "Wavelet Toolbox User's Guide, Version 1: For Use with MATLAB," Math Works, pp. 25-27, 1996.